A Density Functional Study of the Interaction of NCO with Small Copper Clusters

Shuang Zhao,[†] YunLai Ren,[†] JianJi Wang,*[,†,‡] and WeiPing Yin[†]

School of Chemical Engineering, Henan University of Science and Technology, Luoyang, Henan 471003, People's Republic of China, and School of Chemical and Environmental Sciences, Henan Key Laboratory of EnVironmental Pollution Control, Henan Normal University, Xinxiang, Henan 453007, People's Republic of China

Received: July 7, 2008; Revised Manuscript Received: December 4, 2008

Density functional calculations have been carried out for Cu_nNCO^-, Cu_nNCO, Cu_nNCO^+, and Cu_nNCO^{2+} clusters. It was found that for small n, charge state has a strong influence on the NCO location site. The ground states of the neutral and anionic complex clusters have a dominantly planar structure while most of the cationic complex clusters prefer three-dimensional structures. The electrostatic interaction is essential for the Cu−NCO bonding, while covalent interaction through 2π donation strongly enhances the bonding. In neutral and anionic species the N−C bonds are strengthened and the C−O bonds are weakened, while in cationic species all the C−O distances decrease and the N−C distances can be slightly elongated in some cases, which is related to a higher NCO reactivity toward NO and O_2 to form N_2 over the positively charged $Cu_n^{\delta+}$ sites than that over the metallic Cu_n sites.

I. Introduction

The activity of Cu-containing catalysts has attracted considerable attention in the catalytic reduction of NO_x.[1−11] The typical reductants of NO_x are hydrocarbons, CO, and H_2. Isocyanate species (−NCO) have been detected when an equimolar mixture of NO/CO or NO/hydrocarbons is adsorbed on the reduced oxide-supported Cu or Ag catalysts.[1−16] Investigation of the behavior of NCO is of interest because it may be an important intermediate in the lean NO_x reduction to form N_2 and CO_2.[1−16] The reaction of NCO to form N_2 and CO_2 over a catalytic site has been proposed as follows:[1,5,12,13,17]

$$\mathrm{T{-}NCO} \xrightarrow{\mathrm{NO,\ O_2}} \mathrm{N_2 + CO_2 + T,\ T = metal,\ Si,\ or\ Al}$$

$^{15}N_2$ and $^{14}N^{15}N$ were detected as main products of dinitrogen after the reaction of $^{15}NCO + O_2$ and $^{15}NCO + {}^{14}NO + O_2$, respectively.[13] It can be concluded that the cleavage of the N−C bond of NCO is involved in the N_2 formation. Experimental results indicated that the reactivity and stability of the NCO species strongly depend on the metals and/or supports, but the detailed mechanism is still unknown. Recently, in the NO/CO reactions over Cu/SiO_2 and $Cu/SiO_2{-}TiO_2$ catalysts, the active metal site was found to contain both the three-dimensional (3D) and plate-like two-dimensional (2D) metal particles.[18] Experimental investigations of the formation and reactivity of NCO species over Cu-containing catalysts have been performed by IR spectroscopy and mass spectrometry. Solymosi et al. assigned the IR band 2180−2240 cm^{-1} to NCO species bound to Cu, Cu−NCO.[3] Besides, the stability of the NCO species on Cu was found to be much higher than that on Pt and Rh catalysts.[3]

The study of the interaction between the adsorbed NCO species and metal clusters is important for the understanding of the catalytic mechanism. While unambiguous determination of the structure of a small atomic cluster is an almost impossible task from experiments alone, quantum-chemical studies may shed light on the understanding of the catalytic activity of small metal clusters. In the past few years, the adsorption behavior of small molecules, such as propene, CO, H_2, and O_2, on metal clusters has been widely studied in theory.[19−22] It is found that the adsorption behavior of small molecules on metal cluster strongly depends on the charge state and size of the cluster. Theoretical studies of the NCO adsorption on copper clusters have also appeared.[23−25] Castellani et al. investigated the adsorption of NCO over atomic and dimmer copper supported on silica defects.[23] Jian Ming et al. simulated the chemsiorption of NCO on Cu (100) surface using density functional theory (DFT) and a Cu_{14} cluster model.[24] These calculations indicated that the Cu−NCO bonding is largely ionic. However, to our knowledge, a systematic theoretical study of NCO interaction with copper clusters considering the effects of cluster size and charge state is still lacking. In this paper, we present a theoretical study of the binding of NCO on the small Cu_n, Cu_n^+, and Cu_n^- clusters with $1 \le n \le 6$. The geometries of the double charged Cu_nNCO^{2+} clusters were also investigated. The goal of this work is to shed light on the interaction between NCO and Cu clusters as a first step for understanding the role Cu plays in the formation of N_2 and CO_2 from NCO. It is also interesting to study the influence of the different charge states on the structure of a small cluster.

II. Computational Methods

The calculations are carried out by using DFT with the generalized gradient approximation (GGA) and the hybrid GGA functional implemented in the GAUSSIAN 03 package.[26] The Becke's three-parameter hybrid functional (B3LYP)[27] is used in the hybrid DFT, and the Perdew−Wang parametrization (PW91) of the gradient-corrected exchange-correlation energy is used in GGA,[28] for all the calculations in this work. The meta-GGA TPSSTPSS[29] and the hybrid O3LYP[30] were also used for several calculations. The LANL2DZ basis set and the corresponding Los Alamos relativistic effective core potential

* Corresponding author. E-mail: jwang@henannu.edu.cn. Phone/fax: 86-379-64212567.
† Henan University of Science and Technology.
‡ Henan Normal University.

10.1021/jp8059757 CCC: $40.75
Published on Web 01/05/2009

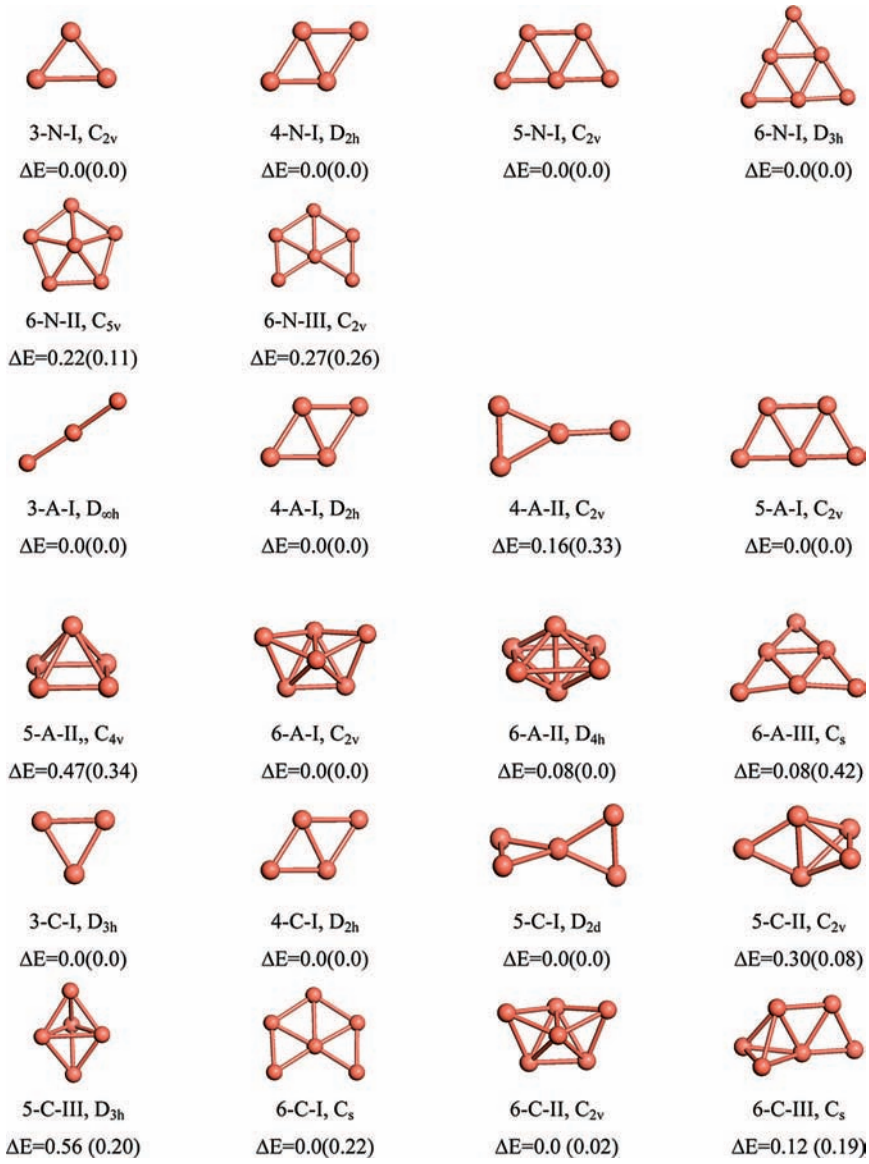

Figure 1. Optimized structures of Cu_n, Cu_n^-, and Cu_n^+ clusters, $n \leq 6$. The sysmmetry point group is indicated. ΔE (in eV) is the excess energy of an isomer as compared to the energy of the most stable isomer. The value of ΔE not in parentheses is calculated with B3LYP, ΔE in parentheses is calculated with PW91PW91.

(RECP)[31] augmented with an *f* polarization function[32] were used for Cu atoms and the 6-311+G* basis set was used for N, C, and O atoms.

Experimental and theoretical investigations have established that NCO was bonded on the metal surface via the N atom.[24,33,34] Thus, the NCO was constrained to N atom binding in the calculations. To have the results of free Cu clusters and NCO binding complex clusters for comparison, we first studied the geometries and properties of the free Cu clusters in the neutral and cationic and anionic charged states. The most stable structures of bare Cu clusters are generally in good agreement with the published literature.[22,35−41] On the basis of the structures of the Cu cluster, wherever the geometry allows it, 1-fold top, 2-fold bridge, and 3-fold face sites were tested upon the binding of NCO on them. Results for bare copper clusters are displayed in Figure 1 and those for complex clusters are displayed in Figures 2−4, together with point group determinations and energetic properties. We studied a very large number of isomers, but we show here the most stable ones (for each cluster size and charge state), together with the less stable isomers whose energy do not exceed that of the most stable isomer by more than 0.30 eV by both B3LYP and PW91PW91 (more structures can be seen in the Supporting Information for the conciseness of the text). For bare copper clusters there are four isomers, 4-A-II, 5-A-II, 6-A-III, and 5-C-III, also displayed in Figure 1. The energy differences between these four structures and the corresponding global minima are beyond 0.30 eV by one or both of the two functionals, but the binding of NCO on them leads to the most stable corresponding complex structures (5-A-II and 5-C-III on PW91PW91, 4-A-II on B3LYP, and 6-A-III on both B3LYP and PW91PW91). In the optimized neutral and charged NCO binding complexes, the Cu−N distances are from 1.8 to 2.1Å. The adsorbates prefer linear or near-linear structures with the N−C−O bond angles mainly changing from 178° to 180°.

All calculations were performed with a (99 590) pruned grid (Ultrafine grid as defined in Gaussian 03). For each structure, the stable method[42] was used to establish a stable wave function. Analysis of vibrational frequencies is performed to make sure the optimized geometries are minima, not transition structures. A scale factor of 0.9614 for B3LYP vibrational frequencies are used as is common.[43]

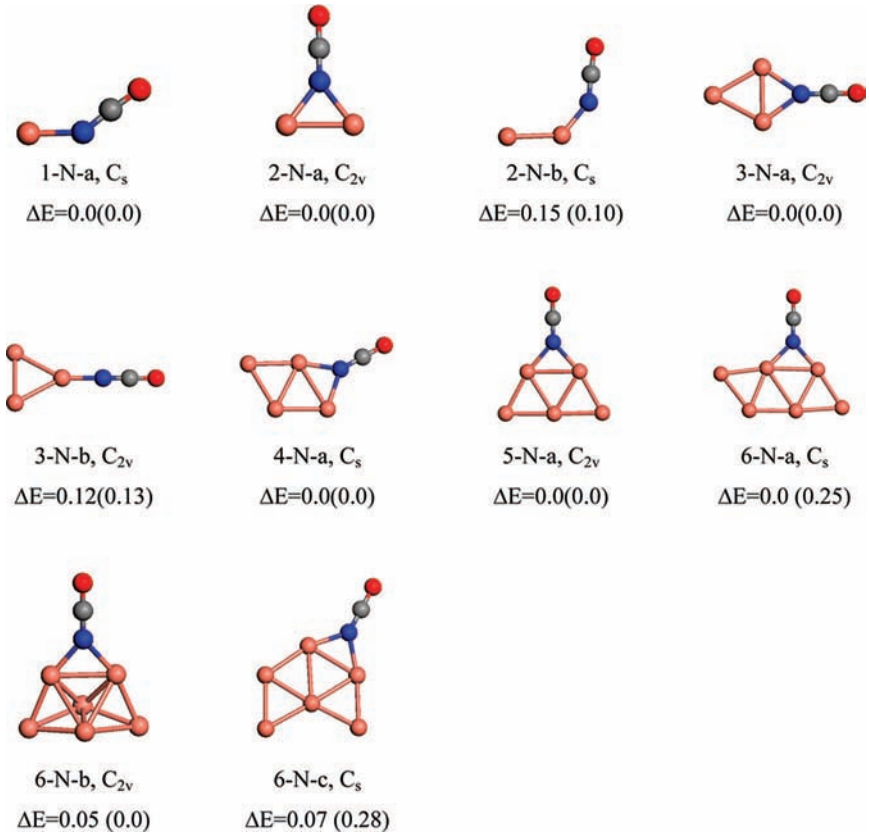

Figure 2. Optimized structures of Cu_nNCO clusters, $n \leq 6$. The sysmmetry point group is indicated. ΔE (in eV) is the excess energy of an isomer as compared to the energy of the most stable isomer. The value of ΔE not in parentheses is calculated with B3LYP, ΔE in parentheses is calculated with PW91PW91.

III. Results and Discussion

Structures and Stability of Bare Copper Clusters. It was established by both extensive experiments and theoretical calculations that Cu_3 has a structure of an isosceles triangle in which one angle is greater than 60°.[39,40] An equilateral triangle and a linear structure were characterized as the most favorable isomers for Cu_3^+ and Cu_3^-, respectively. The rhombus structure was found to be the most stable geometry of the neutral and the anionic and the cationic tetramers, in agreement with most of the previous studies.[22,35−37,39]

The most favorable isomer of Cu_5, as well as Cu_5^-, is characterized as a trapezoidal C_{2v} structure by current DFT calculations, inconsistent with previous GGA calculations.[35−37,39] However, a trigonal bipyramid structure was reported as the most stable isomer for Cu_5 in early molecular-dynamics simulations with use of empirical potential energy functions.[38] In our study a C_{2v} distorted trigonal bipyramid is 0.34 and 0.54 eV less stable than the neutral C_{2v} trapezoidal planar on B3LYP and PW91PW91, respectively. The lowest energy form of Cu_5^+ was characterized to be a D_{2d} structure. This cationic structure can be looked upon as two Cu_2 units cross-linked by a central copper atom. Depending on the dihedral angle between the two Cu_2 units this can also result in an X-shaped butterfly structure with D_{2h} symmetry, which is similar to the case of Ag_5^+.[44] However, with both B3LYP and PW91PW91 calculations this D_{2h} structure is not a minimum. On the other hand, it is only 0.05 eV higher in energy than the D_{2d} structure, indicating that the rotation around the central atom is almost unhindered. A D_{3h} trigonal bipyramid was reported as the most stable Cu_5^+ in refs 35 and 39. However, according to our PW91PW91 calculation the D_{3h} strcture was characterized to be the third stable isomer, and with B3LYP this structure is a second order transition state. A three-dimensional structure with C_{2v} symmetry (5-C-II) was found to be the second stable isomer on both PW91PW91 and B3LYP. The structures of 5-C-I and 5-C-II were probably not considered in earlier GGA calculations of ref 39.

To summarize, for clusters with up to five atoms both B3LYP and PW91PW91 predict the same minimum structures—with only small differences in the respective energies and bond lengths.

As to Cu_6, our study and most of the other theoretical studies indicate a planar D_{3h} structure as the most stable one, followed by the pentagonal pyramid C_{5v} and planar C_{2v} structure. Elbayyari et al. found a rectangular bipyramid to be the global minimum;[38] however, with the present study this structure is a second order transition state. For Cu_6^+, PW91PW91 calculation results in a bicapped tetrahedron as the most favorable isomer, the same structure that Jug et al. found.[35] The global minimum of B3LYP is, however, a near-planar structure with C_s symmetry, in which the two middle Cu atoms are slightly apart from the planar of the four edge atoms. For Cu_6^-, both B3LYP and PW91PW91 calculations found a bicapped tetrahedron as the most favorable isomer, in agreement with earlier LDA and GGA calculations.[22,35,36] The next stable structure on B3LYP is a rectangular bipyramid with D_{4h} symmetry, lying only 0.08 eV higher in energy than the C_{2v} one, while with the PW91PW91 functional, the D_{4h} structure is exactly degenerate with the bicapped tetrahedron. Both the B3LYP and PW91PW91 functionals found a near-planar structure with C_s symmetry as the third stable isomer of the anionic hexamer.

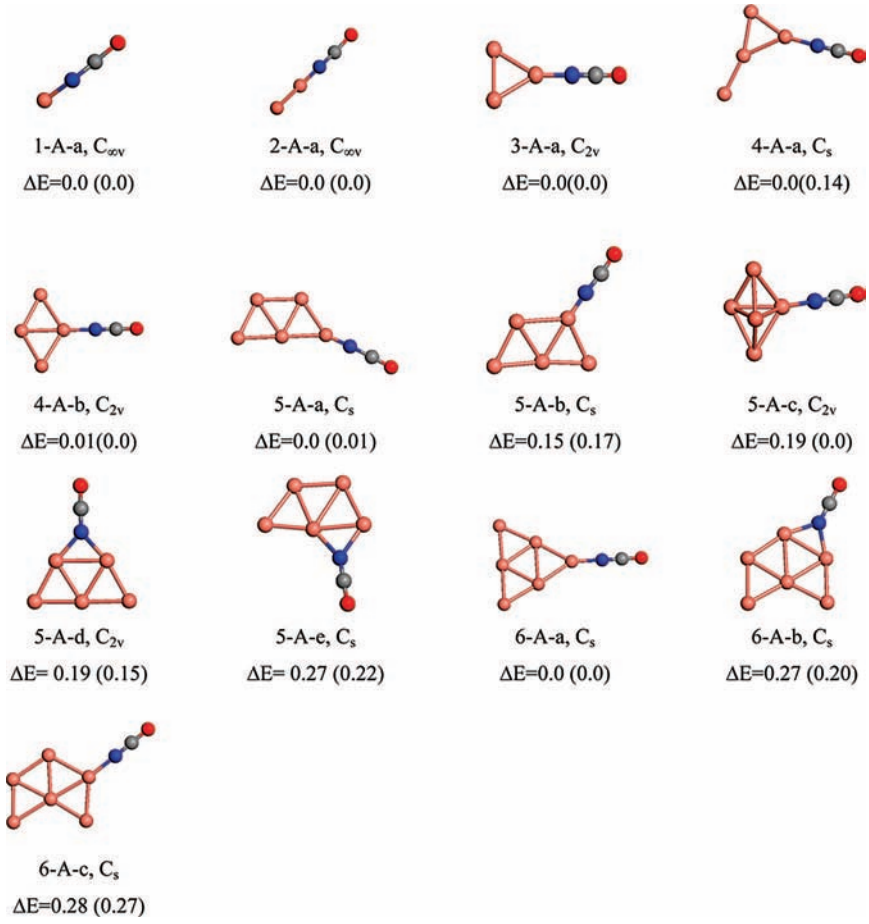

Figure 3. Optimized structures of Cu_nNCO^- clusters, $n \leq 6$. The sysmmetry point group is indicated. ΔE (in eV) is the excess energy of an isomer as compared to the energy of the most stable isomer. The value of ΔE not in parentheses is calculated with B3LYP, ΔE in parentheses is calculated with PW91PW91.

Structures and Stability of Complex Clusters. Figure 2 indicates that from $n = 2$ on, the most stable neutral complexes are all nitrogen on-bridge binding structures. Previous theoretical studies of the chemisorption of NCO on Cu (100) surface also indicated that among different configurations, the binding via the N atom at the bridge site is the most favorable.[24] For the complexes, an important fact observed is that the most stable structure of the Cu_nNCO complex does not always come from that of the lowest energy bare copper cluster plus an attached NCO. With $n \leq 5$, the calculations show that the most stable complexes are related to the most stable Cu_n upon NCO binding, while when $n = 6$, although the planar triangle is characterized as the most stable structure of Cu_6, with NCO adsorbed, a less stable Cu_6 isomer leads to the most stable complex (6-N-a on B3LYP and 6-N-b on PW91PW91).

For anionic clusters, the most stable ones all prefer top adsorption, which could be illustrated with the more "alkali-like" electronic configurations of anionic Cu clusters than neutrals and cations. The binding of NCO to copper clusters can greatly change the geometry of the copper part. For Cu_3NCO^-, the geometry of the copper framework was changed from linear to triangle by the binding of NCO to the middle copper atom of the bare cluster. The finding that the most stable complex cluster does not always come from that of the most stable copper cluster upon NCO binding can also be observed for anions. For Cu_6NCO^-, the most stable structure (6-A-a) is obtained by binding NCO to the near-planar C_s structure of Cu_6^- (6-A-III), but not to the three-dimensional global minimum with C_{2v} symmetry. A similar situation can also be found in Cu_4NCO^- (4-A-a, on B3LYP) and Cu_5NCO^- (5-A-c, on PW91PW91).

Figure 4 displays the most stable structures of the Cu_nNCO^+ clusters. From $n = 2$ on, the most stable Cu_nNCO^+ clusters are all on-bridge binding structures while the on-face binding structures appear as the second or the third stable ones when $n \geq 3$. Notable structural change in the copper framework between Cu_2 and Cu_2NCO^+ can be observed. In Cu_2NCO^+, each copper atom bares a positive charge of $+0.91e$, which is significantly higher than that in the Cu_2^+ cluster. This strong charge repulsion makes the Cu−Cu distance increase from 2.42 Å for Cu_2^+ to 3.31 Å for Cu_2NCO^+ (on B3LYP). In Cu_2NCO, the Cu−Cu bond distance (2.41 Å) has an elongation of only 0.15 Å with respect to its original length in Cu_2 (2.26 Å). Cu_2NCO^- has a linear geometry, in which the Cu−Cu distance is 2.33 Å, shortened by only about "0.06 Å" compared with the bare Cu_2^- (2.39 Å) due to a reduction of electron−electron repulsion by charge redistribution. The most stable Cu_5^+ was characterized as a D_{2d} structure. However, for the B3LYP case, after binding of a NCO, the D_{2d} copper framework was changed to near-planar C_1 structure by the rotation of the two Cu_2 units around the central Cu atom and leads to the most stable complex 5-C-a. For Cu_4NCO^+, the most stable complex 4-C-a was obtained by adding the NCO to a "T" type isomer of Cu_4^+, instead of the most stable bare cluster which is a rhombus. The energy difference between the two most stable bare Cu_6^+ is only 0.02 eV on B3LYP. With the NCO adsorbed, the second stable Cu_6^+ leads to the most stable complex 6-C-a.

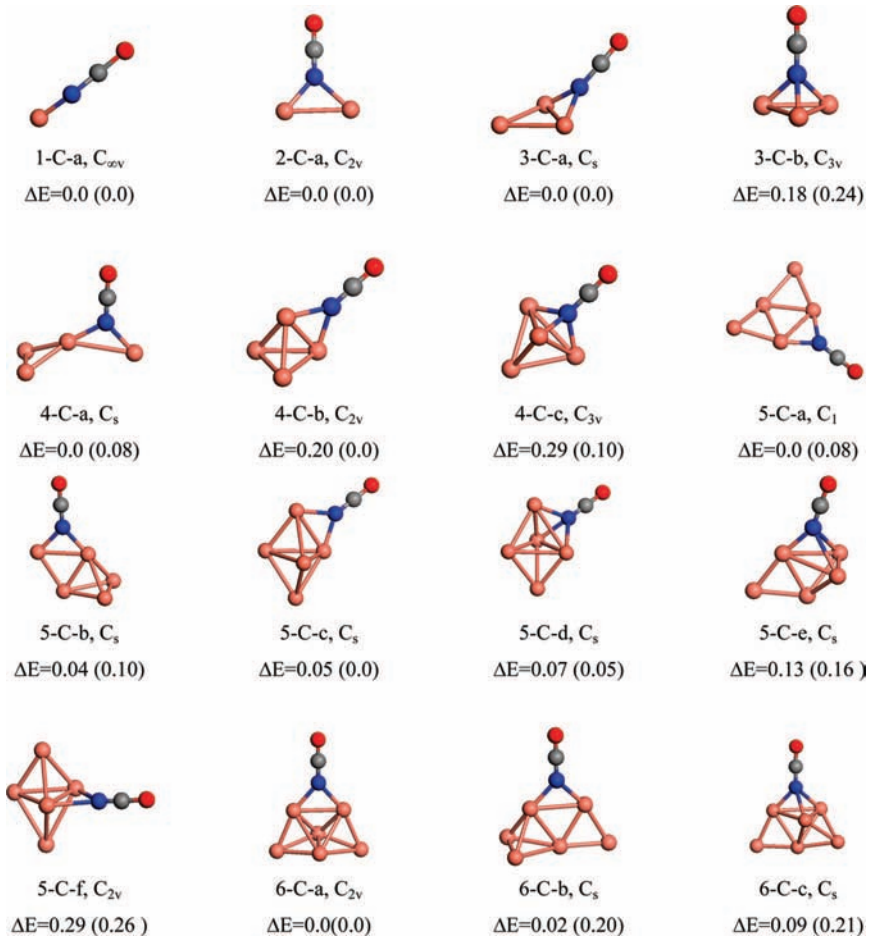

Figure 4. Optimized structures of Cu_nNCO^+ clusters, $n \leq 6$. The sysmmetry point group is indicated. ΔE (in eV) is the excess energy of an isomer as compared to the energy of the most stable isomer. The value of ΔE not in parentheses is calculated with B3LYP, ΔE in the parentheses is calculated with PW91PW91.

It is interesting to find that in general the most stable neutral and anionic complexes prefer planar structures while more 3D structures appear as the most stable ones of the cationic clusters. Natural bond orbital (NBO) population analysis[45] shows that, irrespective of the charge state, electrons transfer from copper clusters to NCO, generally increasing in the order Cu_nNCO^- > Cu_nNCO > Cu_nNCO^+. In cationic clusters, the copper frameworks carry much more positive charges than neutrals and anions, thus with the same number of atoms, a 3D cluster is preferred to get a larger volume than a 2D cluster, which facilitates the distribution of charge over the cluster and reduces the electrostatic energy.

As can be seen from Figures 1−4, B3LYP and PW91PW91 give different results for the most stable structures of Cu_6^+, Cu_6NCO, Cu_4NCO^+, Cu_5NCO^+, Cu_4NCO^-, and Cu_5NCO^-. In these cases the second or the third stable isomer found by B3LYP on PW91PW91 is predicted to be the most stable one. To further test the accuracy of the approach, the meta-GGA TPSSTPSS and hybrid O3LYP methods were used to study the geometries of Cu_4NCO^+ and Cu_4NCO^-. It is interesting to find that O3LYP and B3LYP, both containing Hartree−Fork exchange and the LYP correlation functionals, predict the same global minima, while TPSSTPSS shows an overall agreement with PW91PW91 (both PW91PW91 and TPSSTPSS belong to the Perdew's correlation functionals incorporating the uniform electron gas limit). This indicates that for those isomers with close energies the DFT calculation results are very sensitive to the exchange-correlation functional used. Previous theoretical studies on transition metal clusters[20,44,46] also suggested that in some cases, the search of the global minimum strongly depends on the functionals and the understanding of the geometrical structure of transition metal clusters is a challenging job, since for each cluster there are often several possible isomers connected by a flat potential surface.

N−C and C−O Bond Lengths. For the gas phase NCO, the N−C−O distance is calculated to be 2.40 Å on B3LYP (with an N−C distance of 1.223 Å and a C−O distance of 1.177 Å). This is in good agreement with the experimental value of 2.406 Å.[47] It can be observed from Table 1 that in Cu_nNCO^- clusters the N−C distances are shortened by about 0.033 Å and the C−O distances are elongated by about 0.024 Å on average. A similar but less marked trend can be observed in Cu_nNCO clusters. However, for Cu_nNCO^+ clusters the C−O distances all decrease and the N−C distances increase in some cases (Table 3). PW91PW91 optimization predicts a similar behavior of N−C and C−O distances, with only about 0.01 Å longer in respective bond lengths than those given by B3LYP. The discussions below mainly concentrate on B3LYP calculation results. The data of PW91PW91 can be obtained in the Supporting Information.

The isolated NCO species has a $^2\Pi$ ($7\sigma^2 2\pi^3$) ground state. Even in anionic clusters, the copper atoms connected to N atoms are positively charged, thus forming a local positively charged region in the metal framework. The interaction between NCO and Cu clusters can be mainly divided into two factors: the covalent interaction through 2π donation from metal to NCO, and the electrostatic interaction between metal ions and the lone pair of the N atom. Both factors will strengthen the metal−NCO

TABLE 1: The Results of N−C and C−O Distance (in Å) in Cu_nNCO^- and Cu_nNCO, $1 \le n \le 6$, Computed with B3LYP[a]

	R_{N-C}	ΔR_{N-C}	R_{C-O}	ΔR_{C-O}
NCO	1.223		1.177	
		Cu_nNCO^-		
1-A-a	1.187	−0.036	1.208	0.031
2-A-a	1.187	−0.036	1.207	0.030
3-A-a	1.187	−0.036	1.204	0.027
4-A-a	1.187	−0.036	1.202	0.025
4-A-b	1.186	−0.037	1.205	0.028
5-A-a	1.188	−0.035	1.203	0.026
5-A-b	1.187	−0.036	1.204	0.027
5-A-c	1.186	−0.037	1.204	0.027
5-A-d	1.201	−0.022	1.188	0.011
5-A-e	1.199	−0.024	1.192	0.015
6-A-a	1.188	−0.035	1.203	0.026
6-A-b	1.199	−0.024	1.190	0.013
6-A-c	1.188	−0.035	1.203	0.026
average	1.190	−0.033	1.201	0.024
		Cu_nNCO		
1-N-a	1.202	−0.021	1.183	0.006
2-N-a	1.208	−0.015	1.177	0.000
2-N-b	1.202	−0.021	1.182	0.005
3-N-a	1.207	−0.016	1.179	0.002
3-N-b	1.193	−0.030	1.189	0.012
4-N-a	1.206	−0.017	1.177	0.000
5-N-a	1.207	−0.016	1.177	0.000
6-N-a	1.207	−0.016	1.176	−0.001
6-N-b	1.206	−0.017	1.177	0.000
6-N-c	1.207	−0.016	1.177	0.000
average	1.205	−0.018	1.179	0.002

[a] ΔR is defined as follows: the difference between the bond length (N−C and C−O) in complex clusters and the bond length (N−C and C−O) in free NCO.

TABLE 2: NBO Atomic Charges of NCO (in electron units) in Cu_nNCO^- and Cu_nNCO, $1 \le n \le 6$, Computed with B3LYP[a]

	$q_{(N)}$	$\Delta q_{(N)}$	$q_{(C)}$	$\Delta q_{(C)}$	$q_{(O)}$	$\Delta q_{(O)}$	$q_{(NCO)}$
NCO	−0.28		0.64		−0.36		0
			Cu_nNCO^-				
1-A-a	−0.96	−0.68	0.69	0.05	−0.69	−0.33	−0.96
2-A-a	−0.92	−0.64	0.69	0.06	−0.68	−0.32	−0.91
3-A-a	−0.93	−0.65	0.70	0.07	−0.67	−0.31	−0.89
4-A-a	−0.94	−0.66	0.71	0.07	−0.66	−0.31	−0.89
4-A-b	−0.93	−0.65	0.70	0.07	−0.67	−0.32	−0.90
5-A-a	−0.92	−0.65	0.71	0.07	−0.67	−0.31	−0.89
5-A-b	−0.94	−0.66	0.71	0.07	−0.67	−0.31	−0.90
5-A-c	−0.92	−0.65	0.71	0.07	−0.67	−0.31	−0.89
5-A-d	−1.07	−0.79	0.77	0.13	−0.60	−0.24	−0.90
5-A-e	−1.06	−0.78	0.76	0.12	−0.62	−0.26	−0.92
6-A-a	−0.94	−0.66	0.71	0.07	−0.67	−0.31	−0.89
6-A-b	−1.06	−0.78	0.76	0.12	−0.61	−0.26	−0.92
6-A-c	−0.94	−0.66	0.71	0.07	−0.67	−0.31	−0.90
average[b]	−0.96	−0.69	0.72	0.08	−0.66	−0.30	−0.90
			Cu_nNCO				
1-N-a	−0.99	−0.71	0.75	0.11	−0.57	−0.21	−0.81
2-N-a	−1.16	−0.88	0.80	0.16	−0.54	−0.18	−0.90
2-N-b	−0.93	−0.65	0.75	0.11	−0.55	−0.19	−0.72
3-N-a	−1.13	−0.85	0.79	0.15	−0.55	−0.19	−0.89
3-N-b	−0.99	−0.71	0.75	0.11	−0.59	−0.23	−0.83
4-N-a	−1.12	−0.84	0.79	0.16	−0.54	−0.18	−0.86
5-N-a	−1.11	−0.83	0.80	0.16	−0.54	−0.18	−0.85
6-N-a	−1.11	−0.83	0.80	0.16	−0.54	−0.18	−0.85
6-N-b	−1.10	−0.82	0.80	0.16	−0.54	−0.18	−0.84
6-N-c	−1.11	−0.84	0.80	0.16	−0.54	−0.18	−0.85
average	−1.07	−0.80	0.78	0.14	−0.55	−0.19	−0.84

[a] Δq is defined as follows: the charge difference between the charges of N, C, and O atoms in complex clusters and the charges of N, C, and O atoms in free NCO. [b] The average values are calculated without 1-C-a.

bonding. The 2π MO shows that it is characterized by a bonding orbital between N and C, and an antibonding orbital between C and O (Figure 5). The NBO net charges of free NCO are $-0.28e$ for N, $+0.64e$ for C, and $-0.36e$ for O. After binding, electrons transfer to N and O atoms while C atoms are more positively charged. In anionic complexes, the negative charges of NCO are from $-0.89e$ to $-0.96e$. The high value of the electron transfer indicates the strong 2π donation from metal to NCO, and as a result in anions both the N−C bonding orbital and C−O antibonding orbital will be filled with more electrons, leading to the decrease of N−C distances (about 0.033 Å) and the elongation of C−O distances (about 0.024 Å). A similar behavior of bond lengths related to the 2π donation has been reported in the previous study of NCO adsorption on Cu surface.[24,25]

If we go from anion to neutral, the negative charge of the NCO group decreases by nearly $-0.06e$. Compared with free NCO, the N−C distances decrease by about 0.018 Å on average and the C−O distances increase by 0.012 Å (Table 1). This implies that the 2π donation is less significant in neutral. However, the 2π donation is greatly reduced in cationic clusters. In Cu_nNCO^+ clusters, the positive charges on the C atom increase by about $+0.20e$ and the increase of negative charges on the O atom is within $-0.11e$ compared to that of free NCO (Table 4), while the average increase is $-0.19e$ on O and $+0.14e$ on C for neutrals, and $-0.30e$ on O and $+0.08e$ on C for anions, respectively (Table 2). The 2π MO of NCO is the doubly degenerate π bonds between N and the 2π levels of CO. If we view the −CO as one group, it can be seen from the charge redistribution that this group obtains electron in anions and neutrals, while it loses partial electrons in cations, with respective to −CO in free NCO. Thus, different from anions and neutrals, the reduction of electron in the C−O antibonding orbital causes a distinct decrease of the C−O bond length in cationic clusters.

On the other hand, except for the monomer, in Cu_nNCO^+ clusters there are more electrons concentrated on N atoms than in anions and neutrals ($-1.23e$ versus $-1.07e$ of neutral and $-0.96e$ of anion, on average). This fact, together with the higher positive charge of the C atoms ($+0.84e$ versus $+0.78e$ of neutral and $+0.72e$ of anion, on average), indicates that the cationic Cu clusters present a more relevant polarization effect on the N−C bonds. As a result, in cations the enhancement of the lone pair of N must be more evident and a stronger electrostatic interaction between NCO and metal could be obtained. By the attraction of $Cu_n^{\delta+}$, the electron pairs between N and C are shifted to N atom. The distorting of the electron cloud between N and C is desirable for the weakening of the N−C interaction. In anions and neutrals, the polarization effect is supposed to be negligible and the 2π donation is the dominant factor in the changes of N−C bond lengths. However, in cations, polarization is strengthened as the positive charge on the copper framework is much higher than that in neutrals and anions. The elongation of N−C distances in some cases of Cu_nNCO^+ may be attributed to those cationic copper clusters having stronger ability to polarize N−C bonds and the electron donation to 2π N−C bonding orbital being largely reduced.

The reaction of NCO to form N_2 is related to the N−C bond strength. The influence of the different charge states of clusters on N−C bonds of the adsorbed NCO is also an important topic

TABLE 3: The Results of N−C and C−O Distance (in Å) in Cu_nNCO^+ and Cu_nNCO^{2+}, $1 \leq n \leq 6$, Computed with B3LYP[a]

	R_{N-C}	ΔR_{N-C}	R_{C-O}	ΔR_{C-O}
		Cu_nNCO^+		
1-C-a	1.218	−0.005	1.161	−0.016
2-C-a	1.231	0.008	1.158	−0.019
3-C-a	1.223	0.000	1.158	−0.019
3-C-b	1.235	0.012	1.154	−0.023
4-C-a	1.225	0.002	1.162	−0.015
4-C-b	1.218	−0.005	1.163	−0.014
4-C-c	1.230	0.007	1.158	−0.019
5-C-a	1.215	−0.008	1.164	−0.013
5-C-b	1.218	−0.005	1.164	−0.013
5-C-c	1.218	−0.005	1.163	−0.014
5-C-d	1.227	0.004	1.160	−0.017
5-C-e	1.228	0.005	1.159	−0.018
5-C-f	1.217	−0.006	1.164	−0.013
6-C-a	1.217	−0.006	1.164	−0.013
6-C-b	1.216	−0.007	1.165	−0.012
6-C-c	1.226	0.003	1.160	−0.017
		Cu_nNCO^{2+}		
$CuNCO^{2+}$	1.260	0.037	1.144	−0.033
Cu_2NCO^{2+}	1.267	0.044	1.140	−0.037
Cu_3NCO^{2+}	1.264	0.041	1.143	−0.034
Cu_4NCO^{2+}	1.254	0.031	1.142	−0.035
Cu_5NCO^{2+}	1.247	0.024	1.151	−0.026
Cu_6NCO^{2+}	1.242	0.019	1.148	−0.029

[a] ΔR is defined as follows: the difference between the bond length (N−C and C−O) in Cu_nNCO^{2+} and the bond length (N−C and C−O) in free NCO.

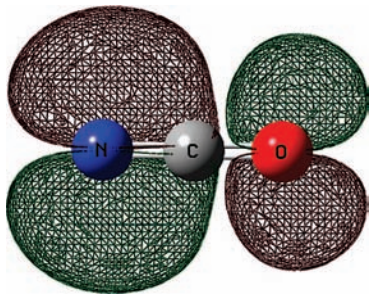

Figure 5. Molecular orbital pictures for 2π MO of NCO.

of this study. From the above discussion, in anionic and neutral clusters the N−C distances become shorter than that in the isolated NCO, which is undesirable for the weakening and breaking of N−C bonds. However, the cationic Cu clusters can slightly increase the N−C distances of NCO in some cases, which is profitable to the weakening of the N−C bond strength. The relatively longer N−C distances in cationic clusters may indicate a higher NCO reactivity toward NO and O_2 to form N_2 over the positively charged $Cu_n^{\delta+}$ sites than that over the metallic Cu_n sites.

In a recent mechanistic study of the HC-SCR (selective catalytic reaction with hydrocarbons as the reducing agent), the Cu^{2+} ion is suggested to play a crucial role in the formation of the final intermediate (Cu−NCO) that results in N_2 formation.[1] Moreover, from the EXAFS (extended X-ray absorption fine structure spectroscopy) data and UV−vis spectra, the structure of $Ag_n^{\delta+}$ clusters on Ag-MFI (Ag-exchanged MFI zeolites) is identified as being Ag_4^{2+} clusters on average in the lean NO_x reduction.[48] Stimulated by this finding, the geometries of the double charged Cu_nNCO^{2+} clusters were also studied in this paper. On the basis of the most stable Cu_nNCO^+ clusters, we optimized the geometries of the Cu_nNCO^{2+} clusters. The stable

TABLE 4: NBO Atomic Charges of NCO (in electron units) in Cu_nNCO^+ and Cu_nNCO^{2+}, $1 \leq n \leq 6$, Computed with B3LYP[a]

	$q_{(N)}$	$\Delta q_{(N)}$	$q_{(C)}$	$\Delta q_{(C)}$	$q_{(O)}$	$\Delta q_{(O)}$	$q_{(NCO)}$
				Cu_nNCO^+			
1-C-a	−0.63	−0.35	0.78	0.15	−0.24	0.12	−0.09
2-C-a	−1.22	−0.94	0.81	0.18	−0.42	−0.06	−0.82
3-C-a	−1.18	−0.91	0.84	0.20	−0.42	−0.06	−0.77
3-C-b	−1.33	−1.05	0.86	0.22	−0.40	−0.04	−0.87
4-C-a	−1.18	−0.90	0.81	0.17	−0.45	−0.09	−0.81
4-C-b	−1.21	−0.94	0.84	0.20	−0.45	−0.09	−0.83
4-C-c	−1.31	−1.03	0.85	0.21	−0.42	−0.06	−0.88
5-C-a	−1.20	−0.93	0.83	0.20	−0.46	−0.10	−0.83
5-C-b	−1.18	−0.90	0.83	0.19	−0.45	−0.10	−0.80
5-C-c	−1.19	−0.91	0.84	0.20	−0.45	−0.09	−0.81
5-C-d	−1.28	−1.00	0.84	0.20	−0.43	−0.07	−0.86
5-C-e	−1.28	−1.00	0.85	0.21	−0.43	−0.07	−0.86
5-C-f	−1.20	−0.92	0.83	0.19	−0.45	−0.09	−0.82
6-C-a	−1.18	−0.90	0.84	0.20	−0.46	−0.10	−0.80
6-C-b	−1.17	−0.89	0.83	0.19	−0.46	−0.11	−0.81
6-C-c	−1.27	−0.99	0.84	0.20	−0.44	−0.08	−0.86
average[b]	−1.23	−0.95	0.84	0.20	−0.44	−0.08	−0.83
				Cu_nNCO^{2+}			
$CuNCO^{2+}$	−0.29	−0.01	0.84	0.20	0.05	0.41	0.59
Cu_2NCO^{2+}	−0.98	−0.70	0.84	0.21	−0.18	0.18	−0.31
Cu_3NCO^{2+}	−1.40	−1.12	0.82	0.19	−0.30	0.06	−0.87
Cu_4NCO^{2+}	−1.40	−1.12	0.88	0.25	−0.30	0.06	−0.82
Cu_5NCO^{2+}	−1.30	−1.02	0.81	0.17	−0.36	−0.01	−0.86
Cu_6NCO^{2+}	−1.36	−1.08	0.88	0.24	−0.34	0.01	−0.83
average[b]	−1.29	−1.01	0.85	0.21	−0.30	0.06	−0.85

[a] Δq is defined as follows: the charge difference between the charges of N, C, and O atoms in Cu_nNCO^{2+} and the charges of N, C, and O atoms in free NCO. [b] The average values are calculated without $CuNCO^{2+}$ and Cu_2NCO^{2+}.

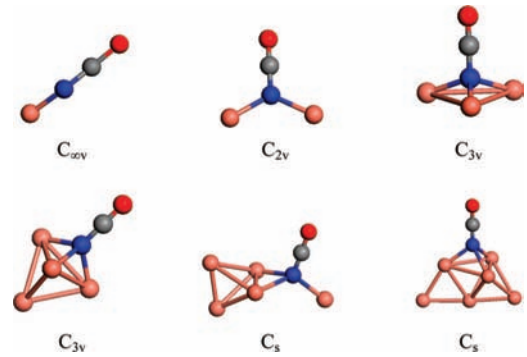

Figure 6. Optimized structures of Cu_nNCO^{2+} clusters, $1 \leq n \leq 6$.

Cu_nNCO^{2+} clusters are listed in Figure 6. From $n = 3$ on, all the optimized Cu_nNCO^{2+} structures are those with the N atoms shared by three Cu atoms and prefer 3D structures. Similar to Cu_nNCO^+, the strong charge repulsion in cationic copper framework has the tendency to pull ions into 3D structures. In comparison with single charged cations, in Cu_nNCO^{2+} the C atom becomes more positive, while electron density on the N atom increases (Table 4). This indicates that a more significant polarization effect on N−C bonds is present in the cases of the dications, which is also reflected in the changes of bond lengths. In the optimized double charged Cu_nNCO^{2+} complexes, the N−C distances are from 1.242 to 1.267 Å, and the C−O distances are from 1.140 to 1.151 Å. It is clear that in Cu_nNCO^{2+} the weakening of N−C bonds and the enhancement of C−O bonds become more evident than that in Cu_nNCO^+. No clear trend of C−O bond distance can be found in cationic clusters, while for N−C distances, it is interesting to notice that smaller cationic clusters often show relatively longer N−C bonds than bigger clusters. For Cu_nNCO^+ clusters with $n \leq 4$, the elongated N−C distances are 1.231 Å for 2-C-a, 1.235 Å for 3-C-b, and 1.230 Å for 4-C-c, while the N−C distances are 1.228 Å for

5-C-e and 1.226 Å for 6-C-c. In the double charged Cu_nNCO^{2+}, the N−C distances decrease with the increasing n, but reach a local maximum at $n = 2$ (1.260 Å for $CuNCO^{2+}$, 1.267 Å for Cu_2NCO^{2+}, 1.264 Å for Cu_3NCO^{2+}, 1.254 Å for Cu_4NCO^{2+}, 1.247Å for Cu_5NCO^{2+} and 1.242 Å for Cu_6NCO^{2+}). Different from other double charged clusters, NCO lost electron to copper in $CuNCO^{2+}$. After adding a Cu atom, NCO receives a negative charge of about $-0.31e$ from metal (Cu_2NCO^{2+}). In other cases of the double charged clusters, the negative charges of NCO slightly change from $-0.82e$ to $-0.87e$, which means that the electron loss of the copper framework is close in those clusters. The situation is similar in Cu_nNCO^+. With the exception of $CuNCO^+$, in other cases the positive charges on copper frameworks are very close. As the cluster size grows, the similar positive charge (with $n \geq 2$ in Cu_2NCO^+ and $n \geq 3$ in Cu_2NCO^{2+}) is distributed within a larger volume of the metal framework so that the positive charge density is smaller. As a result, with increasing cluster size, the polarization ability of cationic metal framework becomes lower and the elongation of the N−C bond becomes smaller. It might be expected that the elongation of N−C bonds will diminish at last if the cluster size grows enough. In other words, the slight weakening of N−C bonds may only happen in very small cationic clusters in experiments.

It may be argued that the different binding sites also result in the different driving forces for the elongation of the N−C bond. The N−C bond lengths obtained from on-face sites (1.235 Å in 3-C-b and 1.230 Å in 4-C-c) often show relatively longer values in comparison with those obtained from on-bridge sites (1.223 Å in 3-C-a and 1.225 Å in 4-C-a). For Cu_5NCO^+ and Cu_6NCO^+, the N−C distances are slightly elongated in the on-face binding isomers (5-C-d, 5-C-e, and 6-C-c), while in on-bridge binding isomers only the shortened N−C bonds can be found. It is additionally supported by more evidently elongated N−C bond lengths in Cu_nNCO^{2+} which are all face coordinated structures.

Binding Energy. The binding energies were calculated with the following formula:

$$E_b = (E + E_{adsorbate}) - E$$

Here $E_{Cu\ cluster}$ is the energy of the naked Cu cluster obtained by energy minimization starting with the same geometry as the Cu framework in the complex cluster removing the adsorbate. For example, in the complex 6-N-a, the Cu cluster has a distorted structure. When the NCO binding energy for this system is calculated, the energy $E_{Cu\ luster}$ used to calculate E_b is the minimum energy of the Cu_6 framework in 6-N-a, which is turned to the structure 6-N-III after relaxation.

The binding energies as a function of cluster size for the most stable Cu_nNCO, Cu_nNCO^-, and Cu_nNCO^+ ($n = 1-6$) calculated by B3LYP functional are displayed in Figure 7. The PW91PW91 binding energies are always larger, by 0.1−0.4 eV (approximately), than those given by the B3LYP functional, while predicting the same trends with B3LYP as a function of cluster size. One can observe the following trends from Figure 7: (1) The clusters with an odd number of electrons bind NCO more strongly than those with an even number of electrons. It is easier for the Cu cluster with an odd number of electrons, which has lower electron affinity (EA), to transfer electron to NCO than the Cu cluster with an even number of electrons. Since the isolated NCO has an unpaired electron at 2π MO and could receive an electron from metal, the interaction between NCO and cluster yields a stronger covalent bond when the copper cluster has an odd number of electrons. (2) The

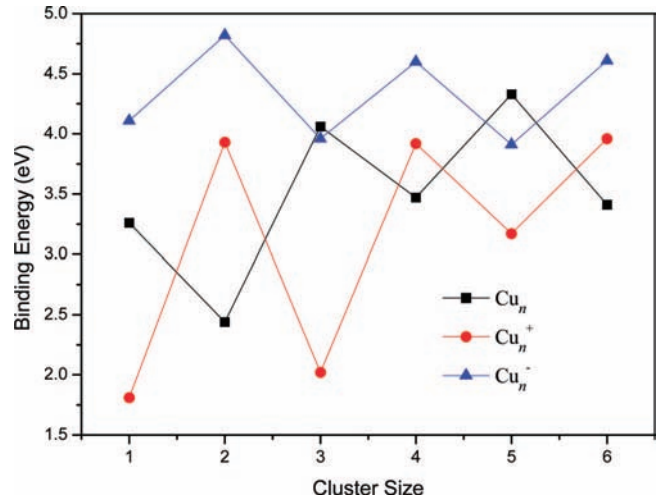

Figure 7. Binding energies as a function of cluster size. A neutral NCO is associated to Cu_n, Cu_n^+, and Cu_n^- clusters, $1 \leq n \leq 6$, computed with B3LYP.

binding energy for the anions is clearly larger than that of the neutral and cationic counterparts except for $n = 3$ and 5. After binding, electrons transfer from metal to NCO with the excess of negative charge concentrated largely in the N atom (mainly from $-0.92e$ to $-1.33e$). As discussed earlier in this paper, both electrostatic interaction and the covalent interaction through 2π donation contribute to the strength of Cu−NCO bonding. The anions have the strongest 2π donation while the cations have the strongest electrostatic interaction. The binding energy ranges for anion, neutral, and cation are 3.91 to 4.82, 2.44 to 4.33, and 1.81 to 3.96 eV, respectively, which is consistent with the order of the 2π donation: anion > neutral > cation. This means that the difference of 2π donation contributes mostly in the different ranges of binding energy for anion, neutral, and cation. On the other hand, the difference of electrostatic interaction is supposed to be rather small and does not cause a substantial difference of binding energy ranges. From both trends, it seems that although the Coulombic interaction is essential for the metal−NCO bonding, covalent interaction through 2π donation strongly enhances the bonding.

NCO has an unpaired electron in the 2π orbital and is very easy to obtain NCO^- with a closed shell. Some experimental studies have suggested that the isocyanate group acts more like an $NCO^{\delta-}$ species than a neutral species when it is adsorbed on a metal surface.[33,34] Thus, the binding energies of NCO^- to Cu_n and Cu_n^+ are also plotted (Figure 8). The attempts to optimize the Cu_5^+ starting with a trapezoidal shape in Cu_5NCO would result in the butterfly structure of Cu_5^+. As mentioned before, the butterfly Cu_5^+ is not a local minimum, but it is very easy for this conformation to isomerize to the D_{2d} structure. Thus the D_{2d} structure was used to calculate the results in Figure 8. The results show that NCO^- binds much stronger to Cu_n^+ than to Cu_n, which is due to a much stronger electrostatic interaction in the former. Notice that the binding energies of NCO^- to copper clusters lose the distinct odd−even oscillation found in the binding between neutral NCO and the bare copper clusters. When the adsorbate is an electron acceptor, the binding energy often oscillates with the EA of the cluster, which has been extensively reported in the literatures.[20,21] However, when the adsorbate binds to a cluster by donating electrons, we could not use the oscillation of EA to predict how the binding energy varies as the cluster size changes. Recently, Metiu et al. studied the adsorption of propene on silver clusters.[19] They found a good correlation between the binding energy of the adsorbate and

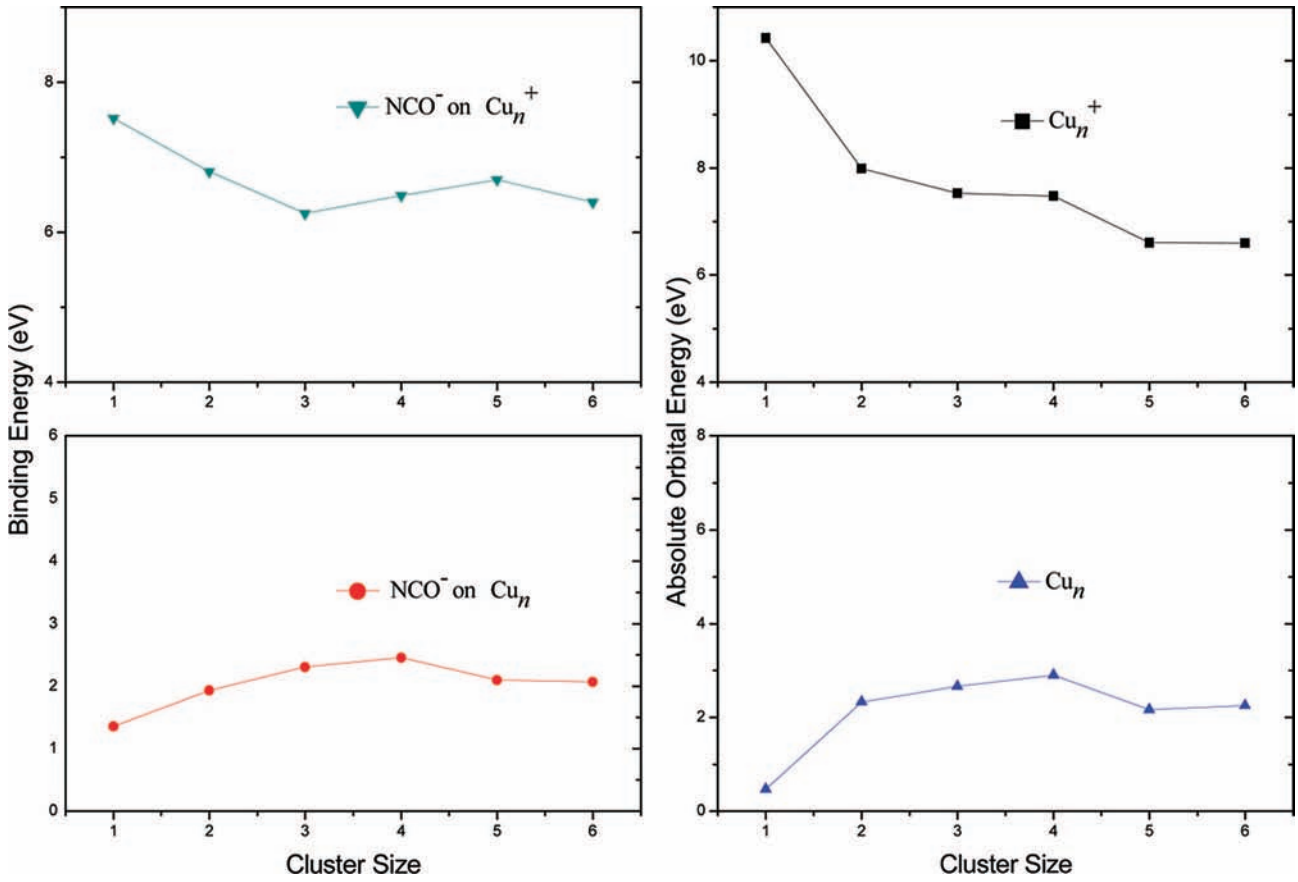

Figure 8. Binding energies of a negative NCO^- and absolute values of the energy of the LUMO of the bare copper clusters as a function of cluster size, computed with B3LYP. The upper and lower rows correspond respectively to the cationic and neutral cluster.

the LUMO energy of the bare silver clusters: the plot of the binding energy of adsorbate versus n is very similar to the plot of the LUMO energy of silver clusters versus n. However, in the cases of NCO^-, the overall correlation between the NCO^- binding energy and the LUMO energy of copper clusters is not that good. For NCO^- binding on Cu_n, the trend of the binding energy is consistent with the energy of the LUMO orbitals with $n \leq 5$ while it failed at $n = 6$. For Cu_n^+ the curve failed from $n = 4$ on. A recent study of CO adsorption on binary-alloy gold clusters also indicated that the CO binding energy does not correlate with bare clusters LUMO energies.[49] Therefore, it implies that the variation of the LUMO energy of the naked cluster may not alone correlate with the E_b trend when the adsorbates denote electrons to clusters. It is likely that multiple interrelated factors, such as the Coulombic interaction and the extent of the overlap of orbitals, all contribute to the observed trend of the binding energy, and the quantitative analysis of these complex interactions is not easy.

Frequency Analysis. The calculated asymmetric and symmetric stretching frequencies of the free NCO are 1918.0 and 1246.6 cm^{-1}, which are only 3 and 20 cm^{-1} underestimated from the experimental values of 1921.3 and 1266.6 cm^{-1}, respectively.[50] According to the data in Table 5, both the asymmetric and symmetric stretching wavenumbers of the adsorbed NCO are blue-shifted compare to those of the free NCO in the neutral and charged complex clusters. For the complex clusters, the calculated asymmetric and symmetric frequencies mainly vary in the range of 2160−2220 and 1276−1343 cm^{-1}, respectively, which is in good agreement with the previous experimental data of refs 3, 18, and 51. Notice that both the asymmetric and symmetric stretching frequencies of NCO are generally decreased as the coordination number of the adsorption site increases. For cationic complexes in Cu_3NCO^+, Cu_5NCO^+, and Cu_6NCO^+, the NCO asymmetric and symmetric stretching

TABLE 5: NCO Asymmetric and Symmetric Stretching Frequencies (in cm^{-1}) of Cu_nNCO^-, Cu_nNCO, Cu_nNCO^+, and Cu_nNCO^{2+}, $1 \leq n \leq 6$, Computed with B3LYP

	asymmetric	symmetric	species	asymmetric	symmetric
1-N-a	2195.1	1328.2	1-C-a	1963.1	1342.7
2-N-a	2191.2	1317.0	2-C-a	2200.2	1286.1
2-N-b	2172.3	1328.1	3-C-a	2214.7	1327.6
3-N-a	2184.3	1315.0	3-C-b	2193.1	1283.0
3-N-b	2223.1	1347.6	4-C-a	2192.6	1293.9
4-N-a	2196.9	1320.1	4-C-b	2207.4	1334.3
5-N-a	2199.3	1320.3	4-C-c	2180.5	1292.7
6-N-a	2198.6	1320.0	5-C-a	2221.0	1338.8
6-N-b	2203.7	1324.2	5-C-b	2210.8	1331.5
6-N-c	2196.0	1319.2	5-C-c	2208.1	1330.4
1-A-a	2193.9	1279.4	5-C-d	2187.4	1296.5
2-A-a	2205.8	1290.4	5-C-e	2189.6	1296.8
3-A-a	2211.9	1300.8	5-C-f	2195.7	1330.1
4-A-a	2213.2	1305.9	6-C-a	2210.8	1330.6
4-A-b	2214.6	1299.4	6-C-b	2210.2	1331.0
5-A-a	2205.6	1301.9	6-C-c	2190.1	1298.4
5-A-b	2205.4	1299.2	$CuNCO^{2+}$	1953.4	1227.6
5-A-c	2217.8	1305.1	Cu_2NCO^{2+}	2075.2	1184.4
5-A-d	2179.0	1297.3	Cu_3NCO^{2+}	2193.7	1202.3
5-A-e	2172.5	1291.3	Cu_4NCO^{2+}	2218.8	1251.6
6-A-a	2203.4	1300.7	Cu_5NCO^{2+}	2177.2	1239.9
6-A-b	2170.9	1292.5	Cu_6NCO^{2+}	2200.4	1276.9
6-A-c	2204.2	1300.2			
exptl		2180−2240;[a] 2180−2220;[b] 1321[c]			

[a] Asymmetric stretching frequencies taken from ref 3. [b] Asymmetric stretching frequencies taken from ref 18. [c] Symmetric stretching frequencies taken from ref 51.

frequencies of on-bridge configurations are about 20−45 cm^{-1} higher than the on-face configurations with the same cluster size. For neutral and anionic complexes, the asymmetric frequencies of on-top configurations are about 30−40 cm^{-1} higher than the on-bridge configurations in Cu_3NCO, Cu_5NCO^-, and Cu_6NCO^-.

IV. Conclusions

In this work, we have systematically studied the interaction between the NCO and the small Cu_n, Cu_n^-, and Cu_n^+ clusters with $1 \leq n \leq 6$. The structures of double charged Cu_nNCO^{2+} were also investigated. It was found that the most stable structure of the complex cluster (Cu_nNCO, Cu_nNCO^-, and Cu_nNCO^+) does not always come from that of the lowest energy bare copper cluster plus an attached NCO and the binding of NCO can greatly change the geometries of the bare copper clusters in some cases. For small n, in addition, charge state is found to have a strong influence on NCO location sites and the geometries of clusters. Generally the neutral and anionic clusters prefer planar structures, while most of the cationic clusters prefer 3D structures. The N on-bridge sites are the most favorable binding sites for Cu_nNCO and Cu_nNCO^+ while the N on-top sites are preferred for Cu_nNCO^-. From $n = 3$ on, the Cu_nNCO^{2+} structures are all those in which the N atom is attached to three Cu atoms.

In neutral and anionic complexes the N−C distances decrease and the C−O distances elongate, indicating that N−C bonds become stronger and C−O bonds become weaker in those clusters. However, in cations the C−O distances all decrease and the N−C distances can be slightly elongated in some cases, suggesting the potential activity of cationic clusters to weaken N−C bonds and strengthen C−O bonds. Compared with Cu_nNCO^+, the elongation of the N−C bond is more evident in Cu_nNCO^{2+}. Our calculation results indicate that the positively charged Cu clusters may have the potential to weaken N−C bonds of NCO, and the tendency to weaken N−C bonds is more evident when the cluster has more positive charge density or the bonding occurs on face (3-fold) sites.

In general the anionic clusters bind NCO more strongly than neutral and cationic clusters and the binding energy shows a remarkable odd−even alternation behavior. The electrostatic interaction is essential for the metal−NCO bonding, while covalent interaction through 2π donation enhances the bonding. The calculated asymmetric and symmetric stretching frequencies of the adsorbed NCO are in good agreement with the experimental data.

Acknowledgment. The project was supported by the Outstanding Talent Program of Henan Province (084200510015) and the Fund for Doctorates of Henan University of Science and Technology.

Supporting Information Available: Tables of net atomic charges of the adsorbates, absoule energies (E), and $\langle S^2 \rangle$ for the neutral and charged Cu_nNCO^-, Cu_nNCO, Cu_nNCO^+, and Cu_nNCO^{2+} ($n = 1-6$) clusters, computed with B3LYP and PW91PW91 functionals. This material is available free of charge via the Internet at http://pubs.acs.org.

References and Notes

(1) Shimizu, K.; Kawabata, H.; Maeshima, H.; Satsuma, A.; Hattori, T. *J. Phys. Chem. B* **2000**, *104*, 2885.
(2) Chi, Y.; Chuang, S. S. C. *J. Catal.* **2000**, *190*, 75.
(3) Solymosi, F.; Bánági, T. *J. Catal.* **1995**, *156*, 75.
(4) Balkenende, A. R.; van der Grift, G. J. G.; Meulenkamp, E. A.; Geus, J. W. *Appl. Surf. Sci.* **1993**, *68*, 161.
(5) Satsuma, A.; Shimizu, K. *Prog. Energy Combust. Sci.* **2003**, *29*, 71.
(6) Li, C.; Bethke, K. A.; Kung, H. H.; Kung, M. C. *J. Chem. Soc., Chem. Commun.* **1995**, 813.
(7) Ukisu, Y.; Sato, S.; Muramatsu, G.; Yoshida, K. *Catal. Lett.* **1992**, *16*, 11.
(8) Gelio, H.; Mudalige, K.; Mills, P.; Trenary, M. *Surf. Sci.* **1997**, *394*, L168.
(9) Oka, H.; Okada, T.; Hori, K. *J. Mol. Catal. A* **1996**, *109*, 51.
(10) Lamsabhi, A. M.; Alcamí, M.; Mó, O.; Yáñez, M.; Tortajada, J.; Salpin, J. Y. *ChemPhysChem* **2007**, *8*, 181.
(11) Bouhlel, O.; Zina, M.; Boughdiri, S.; Tangour, B. *Int. J. Quantum Chem.* **2001**, *84*, 623.
(12) Sumiya, S.; He, H.; Abe, A.; Takezawa, N.; Yoshida, K. *J. Chem. Soc., Faraday Trans.* **1998**, *94*, 2217.
(13) Kameoka, S.; Chafik, T.; Ukisu, Y.; Miyadera, T. *Catal. Lett.* **1998**, *55*, 211.
(14) Sumiya, S.; Saito, M.; He, H.; Feng, Q. C.; Takezawa, N.; Yoshida, K. *Catal. Lett.* **1998**, *50*, 87.
(15) Tanaka, T.; Okuhara, T.; Misono, M. *Appl. Catal., B* **1994**, *4*, L1.
(16) Burch, R.; Breen, J. P.; Meunier, F. C. *Appl. Catal., B* **2002**, *39*, 283.
(17) Solymosi, F.; Völgyesi, L.; Sárkány, J. *J. Catal.* **1978**, *54*, 336. Fokema, M. D.; Ying, J. Y. *J. Catal.* **2000**, *192*, 54.
(18) Boccuzzi, F.; Coluccia, S.; Martra, G.; Ravasio, N. *J. Catal.* **1999**, *184*, 316.
(19) Chrétien, S.; Gordon, M. S.; Metiu, H. *J. Chem. Phys.* **2004**, *121*, 9925.
(20) Zhou, J.; Li, Z. H.; Wang, W. N.; Fan, K. N. *J. Phys. Chem. A* **2006**, *110*, 7167. Zhao, S.; Li, Z. H.; Wang, W. N.; Fan, K. N. *J. Chem. Phys.* **2005**, *122*, 14. Zhou, J.; Li, Z. H.; Wang, W. N.; Fan, K. N. *Chem. Phys. Lett.* **2006**, *421*, 448.
(21) Hagen, J.; Socaciu, L. D.; Roux, J. L.; Popolan, D.; Bernhardt, T. M.; Wöste, L.; Mitrić, R.; Noack, H.; Bonačić-Koutecký, V. *J. Am. Chem. Soc.* **2004**, *126*, 3442. Ding, X. L.; Li, Z, Y.; Yang, J. L.; Hou, J. G.; Zhu, Q. S. *J. Chem. Phys.* **2004**, *121*, 2258.
(22) Cao, Z.; Wang, Y.; Zhu, J.; Wu, W.; Zhang, Q. *J. Phys. Chem. B* **2002**, *106*, 9649. Wang, Y.; Cao, Z.; Zhang, Q. *Chem. J. Chin. Univ.* **2003**, *24*, 675.
(23) Castellani, N. J.; Ferullo, R. M. *J. Mol. Catal. A* **2004**, *221*, 155.
(24) Hu, J. M.; Li, Y.; Li, J. Q.; Zhang, Y. F.; Lin, W.; Jia, G. X. *J. Solid State Chem.* **2004**, *177*, 2763.
(25) Garda, G. R.; Ferullo, R. M.; Castellani, N. J. *Surf. Sci.* **2005**, *598*, 57.
(26) Frisch, M. J.; Trucks, G. W.; Schlegel, H. B.; Scuseria, G. E.; Robb, M. A.; Cheeseman, J. R.; Montgomery, J. A., Jr.; Vreven, T.; Kudin, K. N.; Burant, J. C.; Millam, J. M.; Iyengar, S. S.; Tomasi, J.; Barone, V.; Mennucci, B.; Cossi, M.; Scalmani, G.; Rega, N.; Petersson, G. A.; Nakatsuji, H.; Hada, M.; Ehara, M.; Toyota, K.; Fukuda, R.; Hasegawa, J.; Ishida, M.; Nakajima, T.; Honda, Y.; Kitao, O.; Nakai, H.; Klene, M.; Li, X.; Knox, J. E.; Hratchian, H. P.; Cross, J. B.; Adamo, C.; Jaramillo, J.; Gomperts, R.; Stratmann, R. E.; Yazyev, O.; Austin, A. J.; Cammi, R.; Pomelli, C.; Ochterski, J. W.; Ayala, P. Y.; Morokuma, K.; Voth, G. A.; Salvador, P.; Dannenberg, J. J.; Zakrzewski, V. G.; Dapprich, S.; Daniels, A. D.; Strain, M. C.; Farkas, O.; Malick, D. K.; Rabuck, A. D.; Raghavachari, K.; Foresman, J. B.; Ortiz, J. V.; Cui, Q.; Baboul, A. G.; Clifford, S.; Cioslowski, J.; Stefanov, B.; Liu, B. G.; Liashenko, A.; Piskorz, P.; Komaromi, I.; Martin, R. L.; Fox, D. J.; Keith, T.; Al-Laham, M. A.; Peng, C. Y.; Nanayakkara, A.; Challacombe, M.; Gill, P. M. W.; Johnson, B.; Chen, W.; Wong, M. W.; Gonzalez, C.; Pople *Gaussian03*, Revision C.02; Gaussian Inc.: Pittsburgh, PA, 2003.
(27) Backe, A. D. *J. Chem. Phys.* **1993**, *98*, 5648. Lee, C.; Yang, W. R. *J. Chem. Phys.* **1985**, *82*, 299.
(28) Perdew, J. P.; Chevary, J. A.; Vosko, S. H.; Jackson, K. A.; Pederson, M. R.; Singh, D. J.; Fiolhais, C. *Phys. Rev. B* **1992**, *46*, 6671. Perdew, J. P.; Burke, K.; Wang, Y. *Phys. Rev. B* **1996**, *54*, 16533.
(29) Tao, J.; Perdew, J. P.; Staroverov, V. N.; Scuseria, G. E. *Phys. Rev. Lett.* **2003**, *91*, 146401. Perdew, J. P.; Tao, J.; Staroverov, V. N.; Scuseria, G. E. *J. Chem. Phys.* **2004**, *120*, 6898.
(30) Handy, N. C.; Cohen, A. *J. Mol. Phys.* **2001**, *99*, 403.
(31) Hay, P. J.; Wadt, W. R. *J. Chem. Phys.* **1985**, *82*, 270. Wadt, W. R.; Hay, P. J. *J. Chem. Phys.* **1985**, *82*, 284. Hay, P. J.; Wadt, W. R. *J. Chem. Phys.* **1985**, *82*, 299.
(32) Höllwarth, A.; Böhme, M.; Dapprich, S.; Ehlers, A. W.; Gobbi, A.; Jonas, V.; Köhler, K. F.; Veldkamp, R.; Frenking, G. *Chem. Phys. Lett.* **1993**, *208*, 111.
(33) Jakob, P. *Chem. Phys. Lett.* **1996**, *263*, 607.
(34) Yang, H.; Whitten, J. L. *Surf. Sci.* **1998**, *401*, 312. Hecker, W. C.; Bell, A. T. *J. Catal.* **1984**, *85*, 389.
(35) Jug, K.; Zimmermann, B.; Cataminici, P.; Köster, A. M. *J. Chem. Phys.* **2002**, *116*, 4497.

(36) Matulis, V. E.; Ivashkevich, O. A.; Gurin, V. S. *J. Mol. Struct. (THEOCHEM)* **2003**, *664*, 291.
(37) Jaque, P.; Toro-Labbél, P. *J. Chem. Phys.* **2002**, *117*, 3208.
(38) El-Bayyari, Z.; Oymak, H.; Kökten, H. *Int. J. Mod. Phys. C* **2004**, *15*, 917.
(39) Calaminici, P.; Köster, A. M.; Russo, N.; Salahub, D. R. *J. Chem. Phys.* **1996**, *105*, 9546.
(40) Howard, J. A.; Preston, K. F.; Suteliffe, R.; Mile, B. *J. Phys. Chem.* **1983**, *87*, 536. Crumley, W. H.; Hayden, J. S.; Gole, J. L. *J. Chem. Phys.* **1986**, *84*, 5250. Bauschlicher, C. W., Jr.; Langhoff, S. R.; Partridge, H. *J. Chem. Phys.* **1990**, *93*, 8133.
(41) Calaminici, P.; Köster, A. M.; Vela, A. *J. Chem. Phys.* **2000**, *21*, 1221.
(42) Bauernschmitt, R.; Ahlrichs, R. *J. Chem. Phys.* **1996**, *104*, 9047. Seeger, R.; Pople, J. A. *J. Chem. Phys.* **1977**, *66*, 3045.
(43) Scott, A. P.; Radom, L. *J. Phys. Chem.* **1996**, *100*, 16502.
(44) Weis, P.; Bierweiler, T.; Gilb, S.; Kappes, M. M. *Chem. Phys. Lett.* **2002**, *355*, 355.
(45) Foster, J. P.; Weinhold, F. *J. Am. Chem. Soc.* **1980**, *102*, 7211. Reed, A. E.; Weinhold, F. *J. Chem. Phys.* **1983**, *78*, 4066. Reed, A. E.; Weinstock, R. B.; Weinhold, F. *J. Chem. Phys.* **1985**, *83*, 735.
(46) Lins, J. O. M. A.; Nascimento, M. A. C. *Chem. Phys. Lett.* **2004**, *391*, 9. Belbruno, J. J. *Heteroatom. Chem.* **1998**, *9*, 651.
(47) Misra, P.; Mathews, C. W.; Ramsay, D. A. *J. Mol. Spectrosc.* **1988**, *130*, 419.
(48) Shimizu, K.; Sugino, K.; Kato, K.; Yokota, S.; Okumura, K.; Satsuma, A. *J. Phys. Chem. C* **2007**, *111*, 6481.
(49) Joshi, A. M.; Tucker, M. H.; Delgass, W. N.; Thomson, K. T. *J. Chem. Phys.* **2006**, *125*, 194707.
(50) Copeland, R. A.; Crosley, D. R. *Can. J. Phys.* **1984**, *62*, 1488. Wong, K. N.; Anderson, W. R.; Kotlar, A. J. *J. Chem. Phys.* **1984**, *81*, 2970.
(51) Celio, H.; Mudalige, K.; Mills, P.; Trenary, M. *Surf. Sci.* **1997**, *394*, L168.

JP8059757